

## **Abstract**

The paper shows a model of the nuclear power plant containment used for analysis of its service life. The nuclear power plant is located in Czech Republic in Temelín. The containment consists of prestressed concrete cylindrical structure which is also affected by temperature. The moisture problem was not assumed with respect to age of analysed concrete. The coupled thermo-mechanical analysis had to be performed with respect of these assumptions. In addition to that, the geometry and stress state in the containment have required 3D geometrical model. Generally, the coupled problems have high computing demands especially in the case of 3D problems. This led to modelling only typical section of containment but in 3D and with lot of details. Concrete exhibits very complex behaviour and it is necessary to use several material models to capture major phenomena. In this case, creep, ageing and damage have been modelled. The paper also describes coupling of these models together and describes used damage models. The results from the performed analyses have been compared with measured strains in the reinforcement. There is also comparison of results obtained with usage of different damage models.

**Keywords:** concrete damage, concrete creep, nuclear power plant containment, coupled problem.

## **1 Introduction**

Lot of EU countries have the problem with increasing consumption of electrical energy. In addition to that, there are lot of power plants either coal or nuclear at the end of their projected service life. Usually, the prolongation of service life of the coal power plants is not supported with respect to living environment.

In case of the nuclear power plants, the situation is different because it seems that the production of energy in nuclear power plants will be relatively cheap, sources of atomic fuel are located in relatively stable countries and the problem with nuclear

waste can be solved. That is why the actual operating nuclear power plants are considered for prolongation of their service life.

There are two nuclear power plants in the Czech Republic. The first power plant is in Dukovany and the second is in Temelín. From the above reasons, the question of service life prolongation will rise in the close future. One of the key points will be the prediction of security of concrete containments. Our department was asked for preparation of the analysis focused to the containment in Temelín power plant.

The simulation should capture a period about 30 years with possible extension up to 50 years and one of the requirements was that the results of the analysis should be in good agreement with measurements of strains at the reinforcement. The reinforcement of the containment is organised at all principal directions i.e. there are vertical, radial and side reinforcement. Under these conditions, the used model has to be in 3D in order to capture strains in the reinforcement.

The given containment consists of prestressed concrete cylindrical structure which is also affected by temperature changes caused by operating nuclear reactor. The moisture problem was not assumed with respect to age of analysed concrete. From the material point of view, concrete exhibits very complex behaviour and it is necessary to use several material models to capture major phenomena. In the performed analyses, creep, ageing and damage effects have been taken into account.

## **2 Model of the Containment**

The containment consists of a cylindrical concrete structure. Walls of the containment are prestressed by the system of cables ordered to the crossing loops. In addition to that, there is also reinforcement which is organised at particular principal directions i.e. vertical, radial and horizontal directions.

Several measurement systems have been installed at the containment. One of these systems has been installed at the radial reinforcement. The system measures strains and the results are continuously recorded from the beginning of construction process. Comparison of computed strains in radial direction with measurements should be one of the objectives of performed analyses. Modelling of the reinforcement required fully three dimensional geometry of the containment. Prestressing cables have been another reason for 3D model. They are placed in the system of individual channels. The system of channels together with steel reinforcement led to quite complex geometry and the model of all containment cannot be used due to extremely high computation demands. A characteristic segment of the containment has been used instead of all containment. Figure 1 captures proportion between containment and the meshed segment. The segment width is ~3.0 m, its height is 2.12 m and the thickness is 1.2 m. The segment represents approximately  $7.5^\circ$  of the cylinder. The PE tubes in the cable channels have not been assumed. Distribution of the steel reinforcement and system of tendon channels are depicted in Figure 2.

The model has been meshed by T3D program. Concrete body has been modelled by tetrahedron elements with linear or quadratic approximations, steel reinforcement has been modelled by bar elements with linear or quadratic approximations and cables have not been assumed in geometry. Their effect has been substituted by load

applied in the channels. The mesh density has been increased at the channels neighbour three times compared with rest of the model.

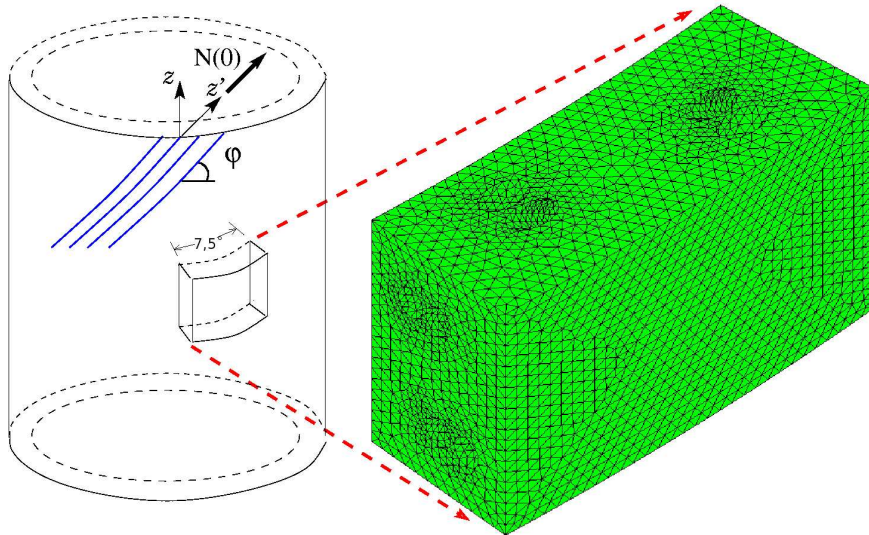


Figure 1: Scheme of the cylindrical segment of the containment

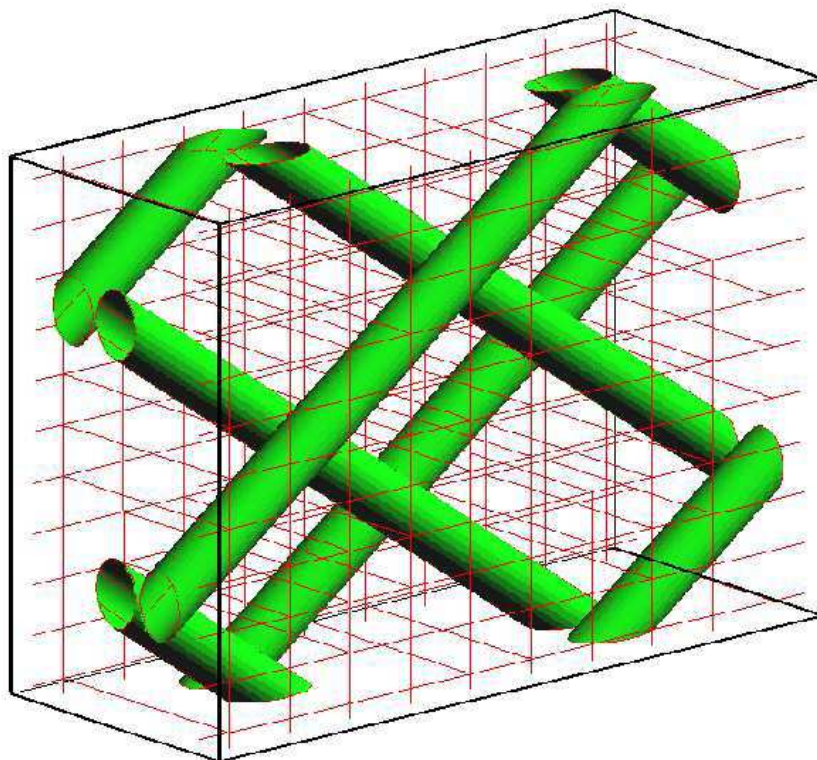


Figure 2: Distribution of the steel reinforcement and system of tendon channels

## 2.1 Mechanical Load

The model have assumed following mechanical loads:

1. Dead weight of the segment
2. Dead weight of the rest of containment applied on the segment top surface
3. Vertical load of top surface caused by prestressing.
4. Direct load in the channels caused prestressing cables – the load is composed from two components. One component has been applied in the normal direction to the channel surface and the other component has been tangential.

Load caused by dead weight has been assumed to be constant in time while the prestressing forces have been prescribed by the time function whose diagram is depicted in Figure 3. The function assumes reduction of prestressing caused by creep and also it assumes increasing prestressing forces due to temperature changes.

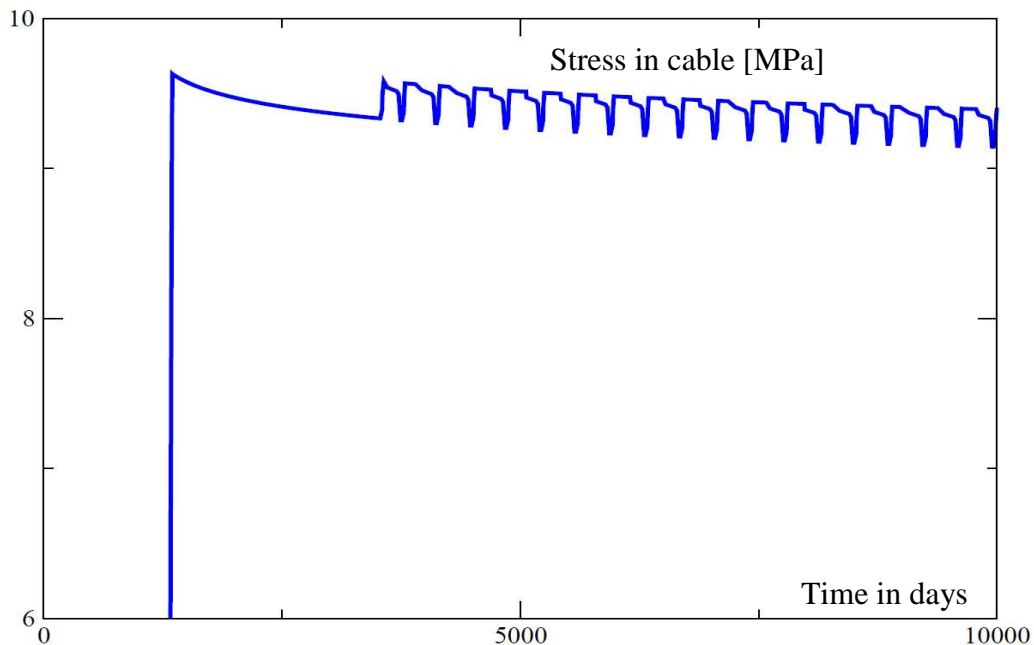


Figure 3: Diagram of stress evolution in the cable

## 2.2 Temperature Load

Temperature load has been determined from the computed distribution of temperature field. The problem of the heat transport has been given by the boundary conditions at the inner and outer segment surface. Applied Dirichlet conditions have been obtained from the idealized course of measured temperatures where one cycle operation/shutdown per year has been assumed. The temperature change at the inner surface has been assumed about 11°C and the change at the outer surface has been assumed about 5°C.

### 3 Solved Problem and Used Material Models

The model of the containment segment has been subjected to the combination of the temperature and mechanical load. Effect of concrete humidity has not been taken into account because of concrete age. Thus the problem led to the thermo-mechanical coupled problem, where changes in the temperature field caused free thermal strains in the mechanical problem. The problem has been solved by the SIFEL code whose source files can be found on <http://mech.fsv.cvut.cz/sifel/>.

The heat transfer has been solved as the nonstationary linear problem with constant parameters. Mechanical behaviour of the segment can be divided into two parts. One part consists of behaviour of the steel reinforcement and the other consists of behaviour of concrete body.

The steel reinforcement has been modelled by bar elements and material properties have been assumed elastoplastic with J2 yield criterion. Modelling of concrete is much more complicated because of its heterogeneity. The model should capture the most important effects only with respect to computer memory and computational speed. In this case, the creep, concrete ageing, damage and thermal strains have been taken into account. Usage of several material models requires usual additive decomposition of the strain tensor. In this case, the decomposition has the following form

$$\boldsymbol{\varepsilon}_{tot} = \boldsymbol{\varepsilon}_e + \boldsymbol{\varepsilon}_d + \boldsymbol{\varepsilon}_{cr} + \boldsymbol{\varepsilon}_{ag} + \boldsymbol{\varepsilon}_{ft}, \quad (1)$$

where

- $\boldsymbol{\varepsilon}_{tot}$  is a total strain
- $\boldsymbol{\varepsilon}_e$  is an elastic component of strain
- $\boldsymbol{\varepsilon}_d$  is a strain component due to damage of concrete
- $\boldsymbol{\varepsilon}_{cr}$  is a creep component of strain
- $\boldsymbol{\varepsilon}_{ag}$  is a ageing component of strain
- $\boldsymbol{\varepsilon}_{ft}$  is a free thermal strain

The creep and ageing have been modelled by the Bazant's B3 model. Details about this model can be found in Bazant [7] and Jirasek [10], details about the implementation in SIFEL and usage in this problem can be found in Krejci [13]. Concrete ageing has been simulated by the increasing of elastic Young modulus. Should be noted that the usual formulation of concrete ageing is written in the incremental form for stress increments

$$\dot{\boldsymbol{\sigma}} = \mathbf{D}_{el}(t) \dot{\boldsymbol{\varepsilon}}, \quad (2)$$

where  $\dot{\boldsymbol{\sigma}}$ ,  $\dot{\boldsymbol{\varepsilon}}$  are stress and strain tensor increments respectively and  $\mathbf{D}_{el}(t)$  stands for elastic stiffness tensor computed from the actual value of the Young modulus. Evolution of the Young modulus is a function of time  $t$ . This form is not suitable for

coupling of creep and damage models. Usually, the damage models are time independent and they are expressed in total strains. The strains caused by ageing should be subtracted from the total strains before the damage computation. In such the case, the total value of  $\boldsymbol{\varepsilon}_{ag}$  can be computed by Equation (3).

$$\boldsymbol{\varepsilon}_{ag,i} = \boldsymbol{\varepsilon}_{tot,i-1} - \frac{E_{i-1}}{E_i} (\boldsymbol{\varepsilon}_{tot,i-1} - \boldsymbol{\varepsilon}_{ag,i-1}), \quad (3)$$

where  $E$  denotes Young modulus, index  $i$  means actual time step and  $i-1$  denotes previous time step.

### 3.1 Damage Models

The scalar isotropic damage model represents the simplest model for damage of concrete. The model should be improved by so called *variable softening modulus technique* in order to avoid mesh dependence. The stress can be written for scalar isotropic damage in the following form

$$\boldsymbol{\sigma} = (1 - \omega) \mathbf{D}_{el} \boldsymbol{\varepsilon}, \quad (4)$$

where  $\omega$  is damage parameter and  $\boldsymbol{\varepsilon}$  is defined as follows

$$\boldsymbol{\varepsilon} = \boldsymbol{\varepsilon}_{tot} - (\boldsymbol{\varepsilon}_{cr} + \boldsymbol{\varepsilon}_{ag} + \boldsymbol{\varepsilon}_{ft}). \quad (5)$$

Evolution law for the damage parameter  $\omega$  can be written in the form of nonlinear equation

$$(1 - \omega) E \kappa = f_t \exp\left(-\frac{\omega h \kappa}{w_f}\right) \quad (6)$$

where  $\kappa$  is equivalent strain norm,  $f_t$  denotes tensile strength of concrete,  $w_f$  is the initial crack opening and  $h$  represents characteristic size of element. In this case, the Mazars equivalent strain norm has been assumed

$$\kappa = \sqrt{\langle \boldsymbol{\varepsilon}_\alpha \rangle \langle \boldsymbol{\varepsilon}_\alpha \rangle}, \quad (7)$$

where  $\langle \boldsymbol{\varepsilon}_\alpha \rangle$  means positive components of principal values of strain tensor. More details about this technique can be found in Jirasek [9] or Koudelka [12].

Taking into account that the object of analysis is in fully 3D stress state, the usage of this model is quite limited because once evolved damage in one direction reduces stiffness at all directions. That was the reason for implementation of an anisotropic or orthotropic damage model. Originally, the anisotropic damage model was

implemented similar to proposed in Papa [11]. The model was derived from Helmholtz free energy

$$\begin{aligned} \rho\psi_{el} = & \frac{3}{2} \left[ (3K - 2G) (\epsilon_v^2 - d \langle \epsilon_v \rangle^2) \right] + G (\mathbf{1} - \mathbf{D}^t)^{1/2} \boldsymbol{\epsilon}^t (\mathbf{1} - \mathbf{D}^t)^{1/2} \boldsymbol{\epsilon}^t : \mathbf{1} + \\ & + G (\mathbf{1} - \mathbf{D}^c)^{1/2} \boldsymbol{\epsilon}^c (\mathbf{1} - \mathbf{D}^c)^{1/2} \boldsymbol{\epsilon}^c : \mathbf{1} \end{aligned} \quad (8)$$

where  $K$  is bulk modulus,  $G$  is shear modulus,  $\epsilon_v$  is the volumetric strain,  $t$  and  $c$  denote tension or compression.  $\mathbf{1}$  is the second order identity tensor. Damage driving forces conjugated to volumetric damage  $d$ , damage tensor for tension  $\mathbf{D}^t$  and damage tensor for compression  $\mathbf{D}^c$  can be derived from Equation (6) by its derivatives with respect to damage parameters:

$$\mathbf{Y}^t = -\frac{\partial(\rho\psi_{el})}{\partial\mathbf{D}^t} = G \boldsymbol{\epsilon}^t \boldsymbol{\epsilon}^t, \quad \mathbf{Y}^c = -\frac{\partial(\rho\psi_{el})}{\partial\mathbf{D}^c} = G \boldsymbol{\epsilon}^c \boldsymbol{\epsilon}^c, \quad y = -\frac{\partial(\rho\psi_{el})}{\partial d} = \frac{9}{2} K \langle \epsilon_v \rangle^2 \quad (9)$$

The tensors  $\mathbf{Y}^t$  and  $\mathbf{Y}^c$  have the same principal directions as  $\boldsymbol{\epsilon}$  and by consequence, both  $\mathbf{D}^t$  and  $\mathbf{D}^c$  also have the same directions. Principal stresses can be derived from Equation (8) by derivatives with respect to strains and the following relation can be obtained

$$\sigma_\alpha = [(3K - 2G)(1 - dH(\epsilon_v))] \epsilon_v + 2G[(1 - H(\epsilon_\alpha))D_\alpha^t - H(-\epsilon_\alpha)D_\alpha^c] \epsilon_\alpha, \quad (10)$$

where  $\alpha$  represents index of principal direction and  $H$  stands for Heaviside function. The model has three sets of three material parameters controlling damage evolution for volumetric and deviatoric damage. Experiences with the model showed that it is possible to reduce this anisotropic model to the orthotropic damage model.

In this case, the orthotropic damage model assumes that the damage evolves at principal directions of strains. In addition, the model takes into account different damage parameters for tension and compression. The basic stress/strain relation is given by

$$\sigma_\alpha = (1 - H(\epsilon_\alpha)D_\alpha^t - H(-\epsilon_\alpha)D_\alpha^c) [(3K - 2G)\epsilon_v + 2G\epsilon_\alpha], \quad (11)$$

Damage parameters  $D$  can be computed either from Equation (12) or Equation (13). Load function defined by Equation (12) was used in Papa [11] originally and it does not take into account characteristic size of mesh element.

$$f_\alpha^\beta = (1 - D_\alpha^\beta) \left[ 1 + A_\beta \left( |\epsilon_\alpha^\beta| - \epsilon_0^\beta \right)^{B_\beta} \right] - 1 \leq 0 \quad (12)$$

In Equation (12),  $\beta$  represents indices  $t$  or  $c$ . Material parameters  $A$  and  $B$  controls the peak stress, slope and shape of the softening branch. Damage threshold

is given by the parameter  $\varepsilon_0$ . The alternative evolution equation can be obtained by a slight modification of Equation (6).

$$(1 - D_\alpha^\beta)E|\varepsilon_\alpha^\beta| = f_\beta \exp\left(-\frac{D_\alpha^\beta h |\varepsilon_\alpha^\beta|}{w_f^\beta}\right) \quad (13)$$

## 4 Results of Performed Analyses

First analyses with the scalar isotropic damage model showed that tensile strength plays a key role. Several analyses with different values of tensile strength of concrete were performed and the results were unrealistic until tensile strength was greater than 3.7 MPa. Lower values of tensile strength led to unrealistic damage of the containment. Experimental value of tensile strength was not measured but there was mean value of the compressive strength obtained from previous experiments. In this case, the value of compressive strength was set to 60 MPa. An approximate value of tensile strength by Czech Technical Standard can be set to 3.5 MPa. That implies that the model with scalar isotropic damage provides the highest limit of concrete damage estimation.

These results led to the conclusion that it will be necessary to perform some experiments with concrete specimens created during containment construction. These experiments have to determine the lowest estimate of the tensile strength and fracture energy.

Another conclusion made from the previous analyses was that there is necessary to use more advanced damage model for concrete. On the other hand, the damage model had to have low computation and memory demands. The above orthotropic damage model appeared to be quite suitable for this case. The values of tensile strength can be set in range 2.0-2.8 MPa and the results were reasonable.

The model of the containment should exhibit good agreement with measured strains at the radial reinforcement. From this point of view, the most important outputs are damage distribution and time dependence of the strains in radial reinforcement. Figure 4 captures damage parameter distribution for isotropic damage model. The tensile strength was assumed 3.75 MPa and the results were obtained after applying 100% of prestressing. The state at the operation beginning can be seen in Figure 5. Similar results are captured in Figure 6 and Figure 7 but the distribution of the crack opening  $w$  is captured. The damage growth can be observed during the prestressing phase especially. Increasing of damage parameter can be also observed at the operation beginning but during particular cycles of shutdowns and operations the damage remains almost unchanged.

Another group of results has been obtained for orthotropic damage model. Figure 8 captures distribution of the tensile damage parameter in the radial direction. The rest of damage parameters have the zero or negligible value. In this case the tensile strength at 2.0 MPa has been assumed. Figure 9 depicts deformed shape of the segment. The shape of the deformed segment corresponds with cracks on the surfaces depicted in Figure 8.

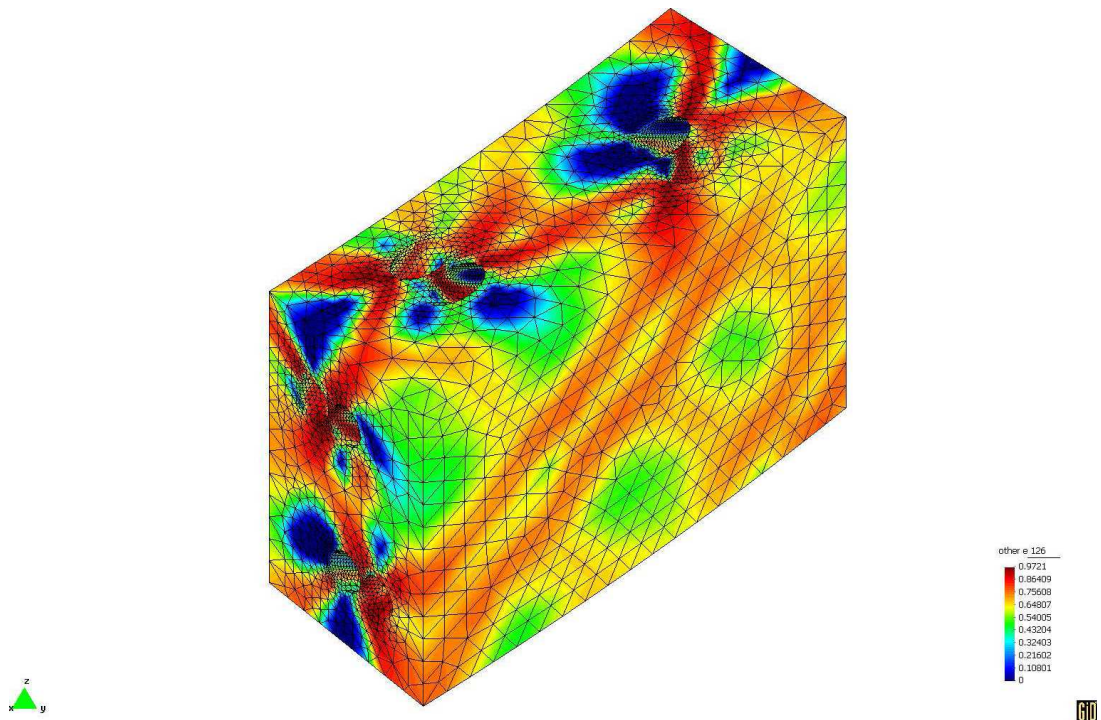


Figure 4: Distribution of damage parameter  $\omega$  for 100% of prestressing

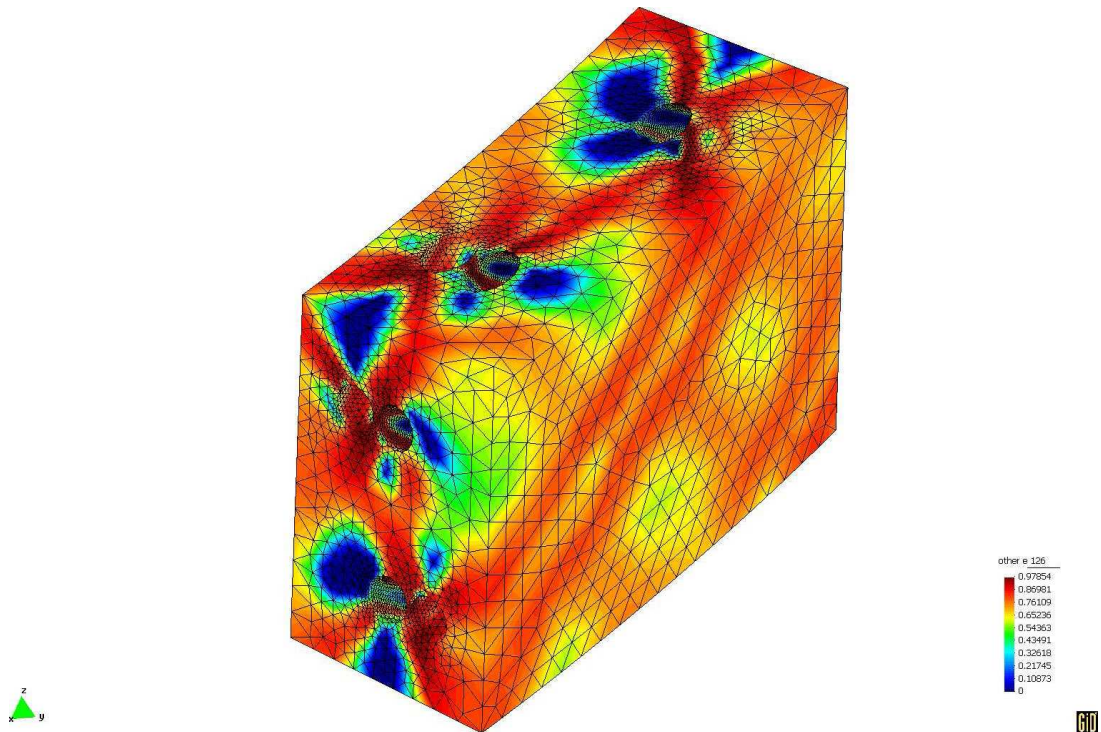


Figure 5: Distribution of damage parameter  $\omega$  for operation beginning

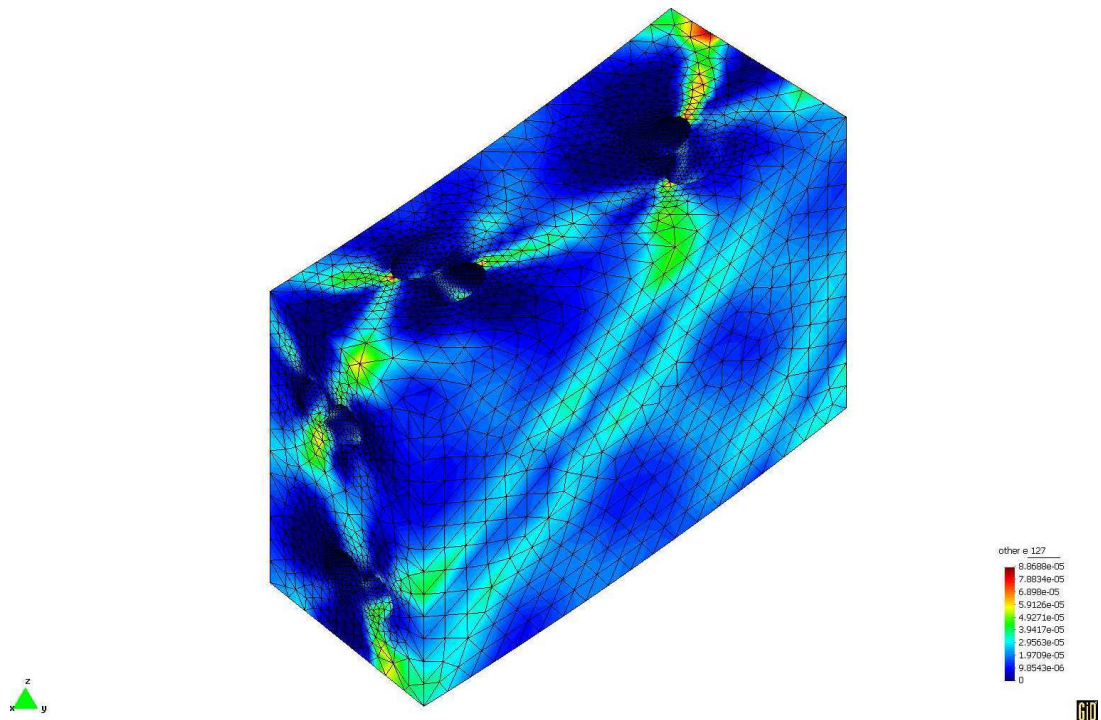


Figure 6: Distribution of crack opening  $w$  for 100% of prestressing

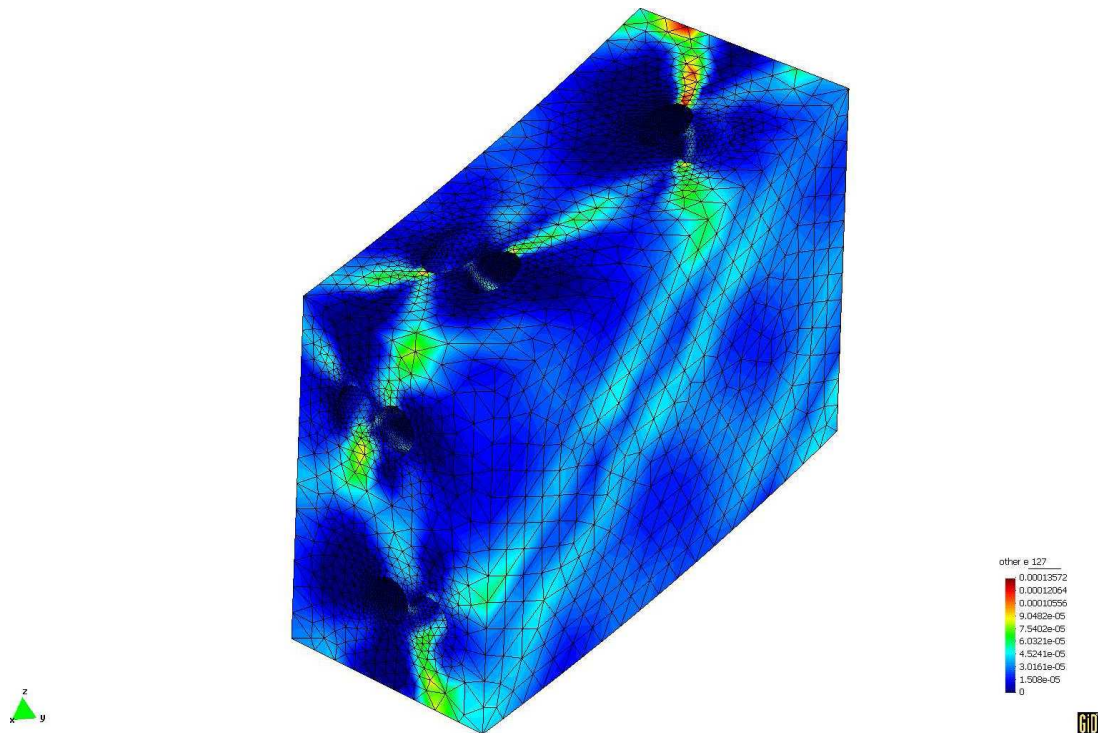


Figure 7: Distribution of crack opening  $w$  for operation beginning

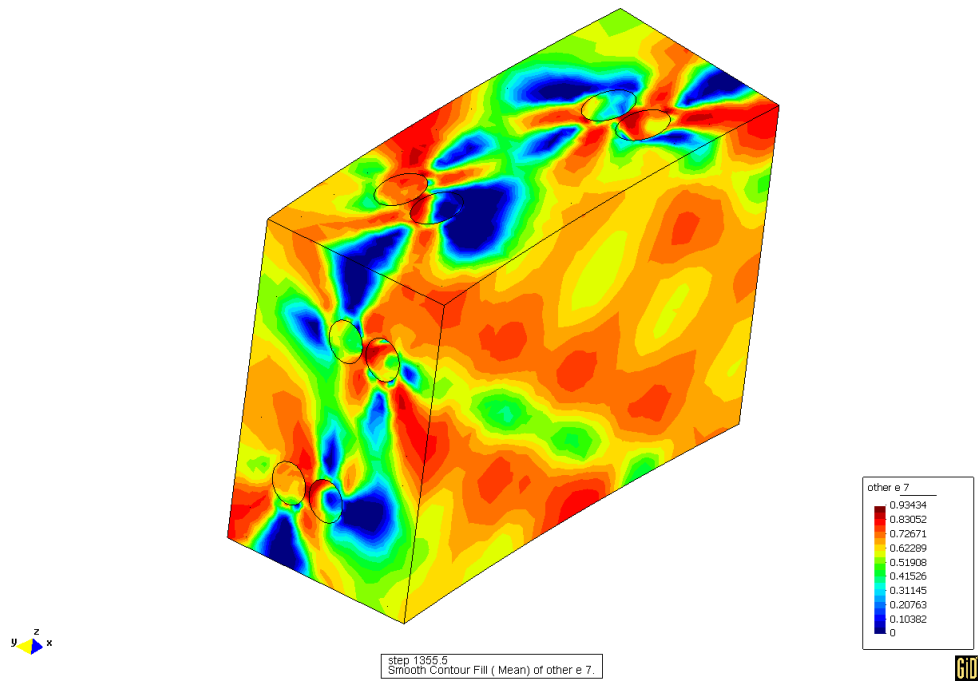


Figure 8: Distribution of damage parameter  $D'$  in radial direction for 100% of prestressing

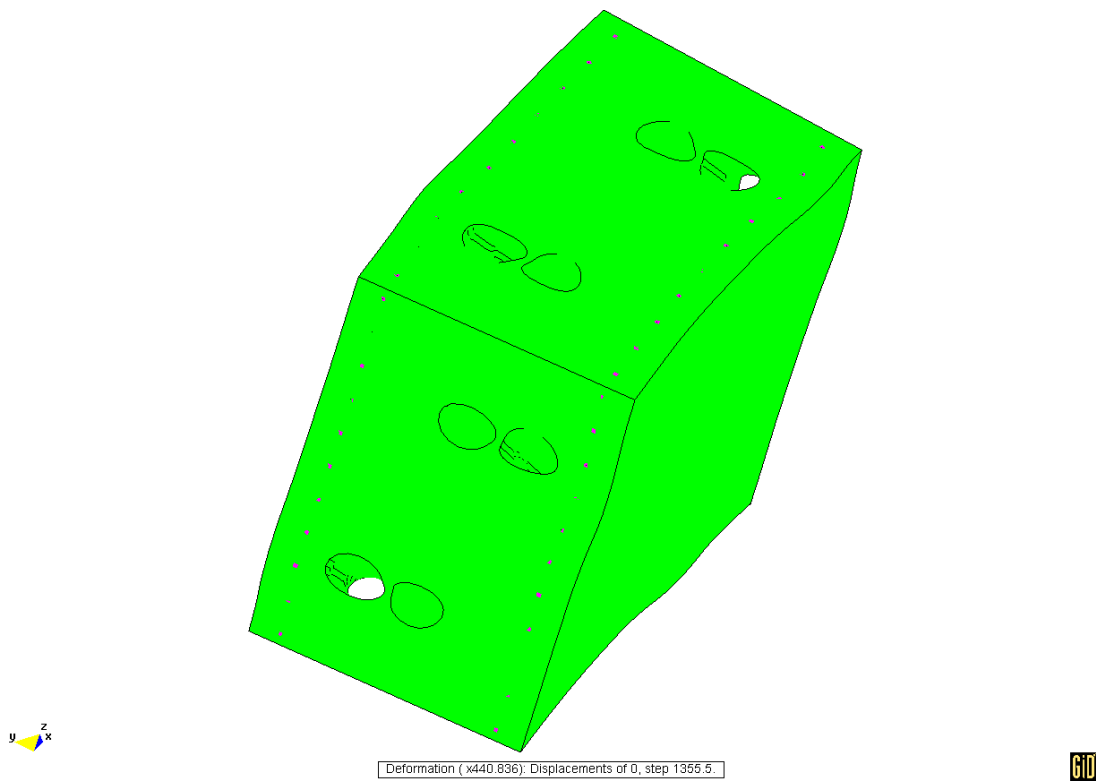


Figure 9: Deformed shape of the segment for 100% of prestressing

The evolution of the strain in the most loaded bar of radial reinforcement can be seen in Figure 10. Due to output data reduction, each two operation/shutdown cycles have been merged together. In the diagram, the dashed red line represents measured strain in the radial reinforcement. The course of the measured strains was simplified and only peak values were connected by this red dashed line. Capturing the trend of the strain evolution during the construction and operation is the main aim and from this point of view, the results in Figure 10 are not acceptable because they differ from measurements significantly since the end of prestressing phase.

The second diagram depicted in Figure 11 has been obtained with the anisotropic damage model. The thick dashed red line represents measured data again. In this diagram, the trend till the beginning of the operation is in good agreement with the measured data but with the increasing number of cycles the trend of computed strain evolution differs from the measurements.

Figure 12 captures the same diagram but for orthotropic damage model. In this case, the tensile strength has been assumed 2.0 MPa. This diagram exhibits the best achieved coincidence with measured data, but evolution of strains differs from measurements since ~4000 days.

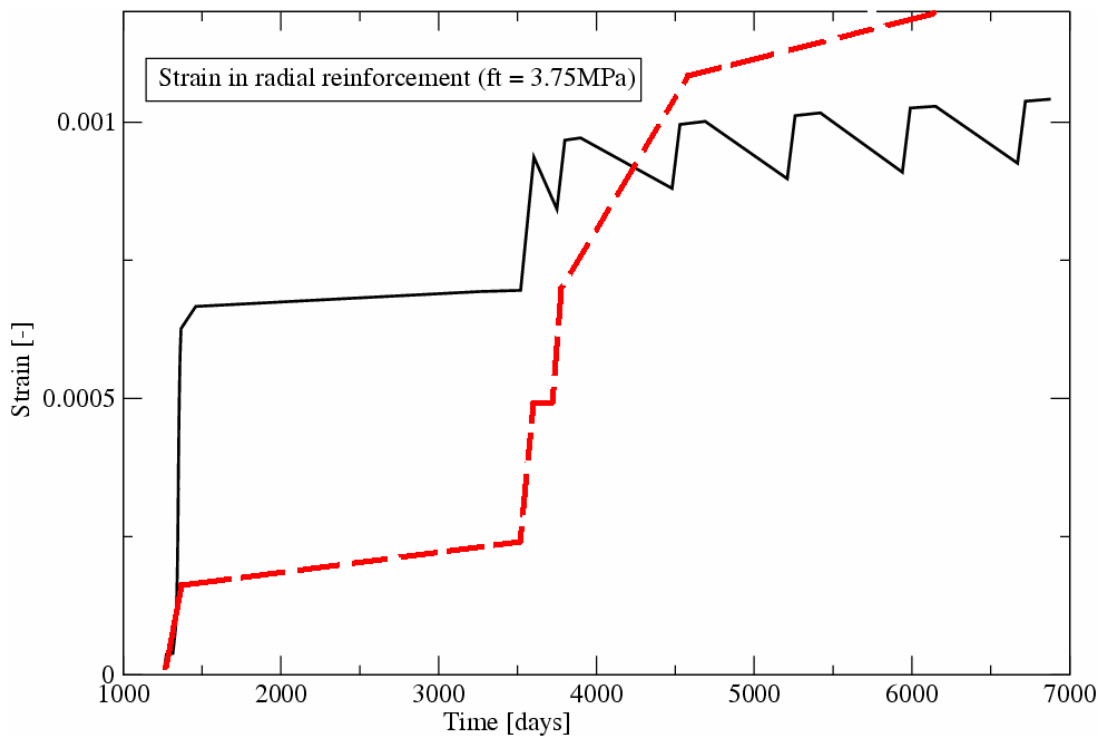


Figure 10: Diagram of strain evolution in the radial reinforcement for the isotropic damage model

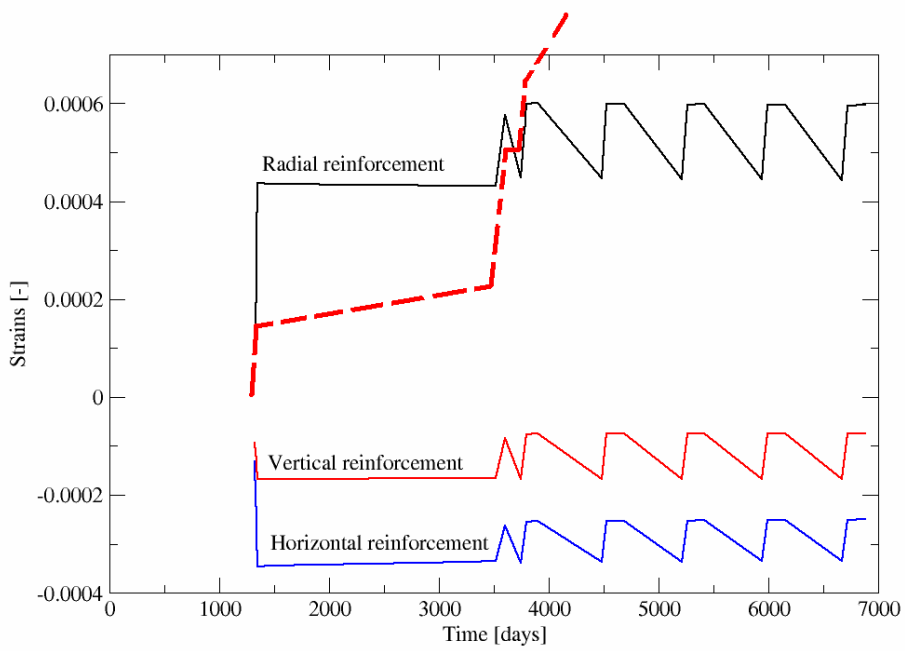


Figure 11: Diagram of strain evolution in the reinforcement for the anisotropic damage model

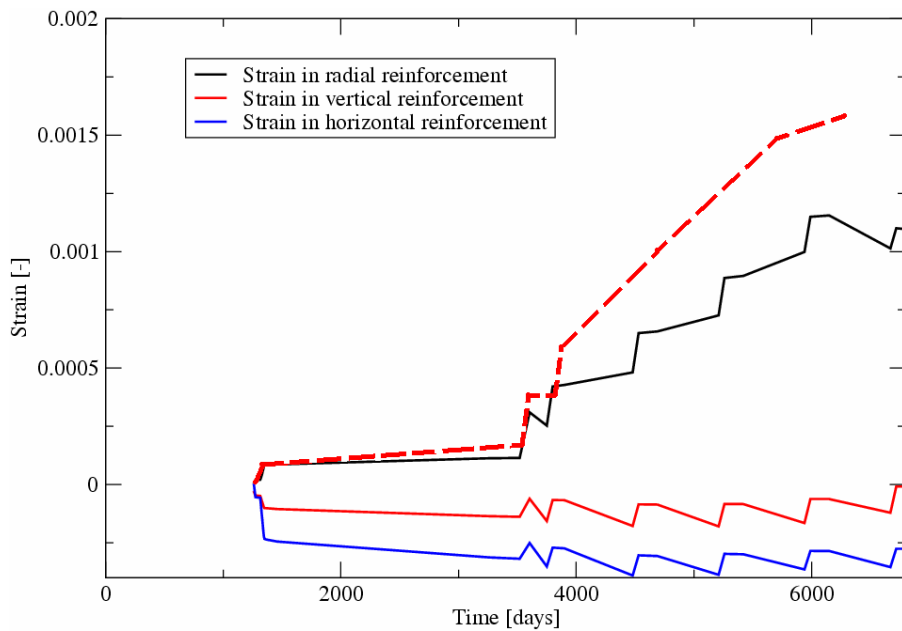


Figure 12: Diagram of strain evolution in the reinforcement for the orthotropic damage model

## 5 Conclusions and Future Development

The model for the service life prediction of the nuclear power plant containment has been prepared. The containment consists of cylindrical concrete structure which is loaded by mechanical and thermal loads. That implies the coupled thermo-mechanical problem had to be solved. In addition, several advanced material models (B3, damage) had to be used in order to capture concrete behaviour. These requirements led to modelling periodic segment (cell) of the containment only. First analyses were concerned on capturing trends of the containment behaviour and identifying of important processes in concrete which have to be modelled. Following conclusions can be made from the results of the performed analyses:

1. Isotropic damage model cannot be used in this case. Results obtained with this model showed unrealistic degree of damage and course of the strain in the radial reinforcement differed since the prestressing phase.
2. Anisotropic damage model could be used, tensile strength of concrete can be chosen in reasonable range, but calibration of the model is more complicated than for the orthotropic model.
3. The orthotropic damage model has been implemented and it provided good results. The model has less material parameters and it can be calibrated easier than the anisotropic model. Good agreement with the measured data has been achieved with this model especially at the interval from the beginning to ~4000 days. Agreement has to be improved in the rest of interval. It can be achieved by the other calibration or by addition another material model capturing other phenomena in concrete (fatigue, temperature dependence of material parameters).
4. Key point of the future analyses will be accessibility of the material parameters. From this point of view, several experiments on concrete specimens have to be performed in order to obtain tensile strength and fracture energy.
5. Computations of the model took lot of computer time and parallelization of the SIFEL code has to be performed. Actually, some coupled problems can be solved in parallel way but there is still something to do for this kind of analysis.

## Acknowledgements

This outcome has been achieved with the financial support of the Ministry of Education, Youth and Sports of the Czech Republic, project No. 1M0579

## References

- [1] R.W. Lewis, B.A. Schrefler, "The finite element method in static and dynamic deformation and consolidation of porous media", John Wiley & Sons, Chichester-Toronto (492), 1998.

- [2] G. Pijaudier-Cabot, L. Jason, “Continuum damage modeling and some computational issues”, RFGC – 6/2002, Numerical Modelling in Geomechanics, p. 991-1017, 2002.
- [3] B. Sluys, “Constitutive modeling of concrete and nonlinear computational dynamics”, RFGC – 7-8/2003, Geodynamics and Cycling Modelling, p. 911-973, 2003
- [4] R. de Borst, P. Nauta, “Non-orthogonal cracks in a smeared finite element model”, Eng. Comp., 2(1), p. 35-46, 1985.
- [5] Z.P. Bazant, T.B. Belytschko, T.P. Chang, “Continuum theory for strain-softening”, ASCE J. Eng. Mech., 110, p. 1666-1692, 1984
- [6] G. Pijaudier-Cabot, Z.P. Bazant, “Nonlocal damage theory”, ASCE J. Eng. Mech., 113, p. 1512-1533, 1987
- [7] Z.P. Bazant, S. Baweja, “Justification and Refinements of Model B3 for Creep and Shrinkage. Updating and Theoretical Basis”, Mater. Struc. 28, 1995, p. 44-50, 1995
- [8] Z. Bittnar, J. Šejnoha, “Numerical methods in structural mechanics”, ASCE Press USA and Thomas Telford UK, 1996
- [9] M. Jirásek, “Numerical Modeling of Deformation and Failure of Material”, Czech Technical University, Prague, 1998
- [10] M. Jirásek, Z.P. Bazant, “Inelastic Analysis of Structure”, John Wiley & Sons, Chichester-Toronto, 2001
- [11] E. Papa, A. Taliercio, “Anisotropic Damage Model for the Multiaxial Static and Fatigue Behaviour of Plain Concrete”, Engineering Fracture Mechanics, Vol. 55, No. 2, Elsevier Science Ltd., 1996
- [12] T. Koudelka, T. Krejčí, J. Šejnoha, “Modelling of Sequential Casting Procedure of Foundation Slabs”, Proceedings of the Twelfth International Conference on Civil, Structural and Environmental Engineering Computing, Stirling: Civil-Comp Press Ltd, 2007
- [13] T. Krejčí, T. Koudelka, J. Šejnoha, “Computer simulation of concrete structures under cyclic temperature loading”, Proceedings of the Twelfth International Conference on Civil, Structural and Environmental Engineering Computing, in print, Stirling: Civil-Comp Press Ltd, 2009